

Original Article

Combining serum biomarkers and MRI radiomics to predict treatment outcome after thermal ablation in hepatocellular carcinoma

Ludong Zhao^{1,2*}, Jing Wang^{3*}, Jinna Song¹, Fenghua Zhang⁴, Jinghua Liu^{1,2}

¹Jinzhou Medical University Postgraduate Training Base of Linyi People's Hospital, Linyi 276000, Shandong, P. R. China; ²Department of General Surgery Center, Linyi People's Hospital, Linyi 276000, Shandong, P. R. China; ³Department of Radiology, Linyi People's Hospital, Linyi 276000, Shandong, P. R. China; ⁴Department of Operating Room, Linyi People's Hospital, Linyi 276000, Shandong, P. R. China. *Equal contributors.

Received February 27, 2024; Accepted February 9, 2025; Epub March 15, 2025; Published March 30, 2025

Abstract: Objective: To investigate the predictive value of serum alpha-fetoprotein (AFP), lectin-reactive alpha-fetoprotein (AFP-L3), and multimodal magnetic resonance imaging (MRI) radiomics in forecasting therapeutic efficacy and prognosis following radiofrequency ablation (RFA) in patients with hepatocellular carcinoma (HCC). Methods: A retrospective analysis was conducted on HCC patients who underwent RFA between January 2019 and December 2023. Clinical and radiologic features of HCC were analyzed. A predictive model was developed using clinical data and radiomic features collected before surgery, with the goal of predicting prognosis after RFA. The predictive performance of the model was evaluated using AUC values in both training and validation cohorts. Results: A total of 298 HCC patients were included in the study, divided into a good prognosis group (n=145) and a poor prognosis group (n=153). Serum AFP and AFP-L3 levels were significantly higher in the poor prognosis group (P=0.007 and P=0.02, respectively). Independent predictive factors included: AFP-L3 (95% CI -1.228, -1.1.61; P<0.001), AFP (95% CI 0.017, 0.036; P<0.001), intratumoral hemorrhage (95% CI 0.380, 0.581; P<0.001), peritumoral arterial tumor enhancement (95% CI 0.193, 0.534; P<0.001) and low signal intensity around liver and gallbladder tumors (95% CI 0.267, 0.489; P<0.001). The combined clinical-radiological-radiomics model demonstrated superior predictive performance, with AUC value of 0.897 in the training set and 0.841 in the validation set, outperforming individual models and sequences. Conclusion: The integrated clinical-radiological-radiomics model showed excellent predictive performance for the prognosis of HCC patients undergoing RFA, surpassing individual models. Key predictors included serum AFP, AFP-L3 levels, intratumoral hemorrhage, and peritumoral low signal intensity. This multimodal approach offers a promising tool for individualized prognostic assessment and improved clinical decision-making.

Keywords: Serum AFP, AFP-L3, multimodal magnetic resonance imaging radiomics, hepatocellular carcinoma, thermal ablation, therapeutic efficacy, predictive

Introduction

Primary liver cancer is one of the most common malignancies globally, ranking as the sixth most common cancer and the fourth leading cause of cancer-related death worldwide in 2018 [1]. In recent years, the incidence of liver cancer has been rising across most countries [2]. In China, primary liver cancer is the fourth most common malignancy and the second leading cause of cancer-related death, with hepatocellular carcinoma (HCC) accounting for 85%-90% of cases [3-5]. Thermal ablation, including radiofrequency ablation (RFA) and

microwave ablation (MWA), has emerged as a minimally invasive and effective treatment modality, particularly for patients who are ineligible for surgical resection [6]. Despite its clinical advantages, post-ablation outcomes remain highly variable, highlighting the need for reliable methods to assess therapeutic efficacy and predict tumor recurrence.

RFA uses radiofrequency energy to induce coagulative necrosis in tumor tissue, effectively killing tumor cells [7, 8]. RFA is known for its precision, minimal trauma, few complications, and strong repeatability, making it widely utilized in

clinical practice [9]. However, despite its efficacy, post-ablation recurrence and treatment failure remain significant challenges. Previous studies have explored predictive models based on clinical, imaging, or molecular data to assess treatment outcomes, but these approaches often have limitations [10-12]. Many studies rely on single data modalities, such as serum biomarkers or imaging features, which fail to capture the full complexity of tumor biology and its microenvironment [13, 14]. Additionally, most imaging-based studies focus on visual assessment or basic imaging, neglecting the potential of advanced radiomics analysis to quantify tumor heterogeneity and peritumoral characteristics [15, 16]. Similarly, serum biomarker studies are often limited by their inability to incorporate spatial information about the tumor and surrounding tissues. These limitations reduce the accuracy and clinical value of existing predictive models.

Tumor markers offer the advantages of convenient detection and high sensitivity compared to imaging examinations. Previous studies have demonstrated the significance of laboratory indicators and clinical characteristics, such as alpha-fetoprotein (AFP), lectin-reactive alpha-fetoprotein (AFP-L3), tumor size, tumor number, and Child-Pugh liver function classification, in monitoring the therapeutic effect of hepatocellular carcinoma (HCC) [17]. Among these, AFP is the most well-established tumor marker, widely used alongside imaging examinations to assist in the clinical diagnosis and treatment of liver cancer after radiofrequency ablation (RFA). Although serum AFP is highly specific for diagnosing HCC, its sensitivity is low, and it has a high false positive rate, leading to misdiagnosis or missed diagnoses. Therefore, relying solely on AFP for evaluating therapeutic efficacy and prognosis after liver cancer RFA is insufficient, particularly for patients with preoperative serum AFP levels below 400 ng/mL, where AFP testing alone has limited reference value [18, 19].

In recent years, radiomics analysis of medical images has emerged as a promising research area, with broad clinical applications [20, 21]. By using logistic regression and machine learning algorithms, quantitative imaging features reflecting tumor microenvironment characteristics - such as cellular structure, necrosis, angio-

genesis, and extracellular matrix deposition - can be extracted and analyzed. These features provide higher-dimensional imaging data than those observed through visual inspection by human experts [22]. Radiomics methods derived from various medical images have gained attention as non-invasive diagnostic tools for assessing post-RFA outcomes in liver cancer. Unlike manual feature extraction, computer algorithms enable the extraction of more 2D and high-dimensional imaging features, providing clinicians with more scientifically valuable objective data for preoperative planning and personalized treatment selection [23, 24].

This study addresses these gaps by integrating serum biomarkers and MRI-based radiomics features, leveraging their complementary strengths to develop a comprehensive predictive model for outcomes after RFA. By incorporating radiomics-derived tumor and peritumoral features alongside biomarker dynamics, this approach offers a novel, multidimensional perspective on tumor behavior. To the best of our knowledge, few studies have systematically combined serum biomarkers with MRI radiomics to predict post-RFA outcome in HCC. The novelty of this study lies in its integrative design, advanced radiomics workflow, and rigorous validation of the proposed model. This may allow personalized treatment planning and improved prognosis in HCC patients.

Therefore, this study aimed to investigate the predictive value of serum AFP, AFP-L3, and multimodal MRI radiomics in forecasting the therapeutic efficacy and prognosis after RFA in HCC patients. Ultimately, the goal is to establish a predictive model that provides an early, accurate, and non-invasive prognosis after RFA, offering a valuable reference for clinical diagnosis, treatment, and follow-up.

Materials and methods

Patient selection

A total of 298 patients with HCC from Linyi People's Hospital were retrospectively selected as study subjects between January 2019 and December 2023. All patients met the diagnostic criteria for HCC as outlined in the Guidelines for the Diagnosis and Treatment of Hepatocellular Carcinoma (2019 edition) issued by the

Serum biomarkers and MRI for hepatocellular carcinoma

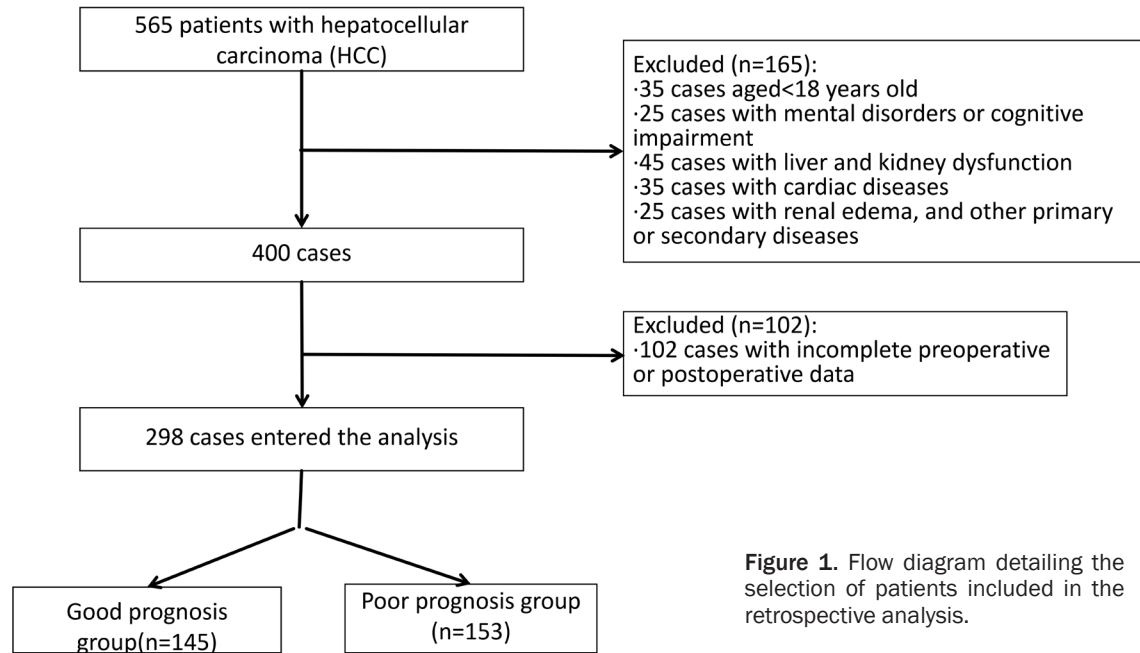


Figure 1. Flow diagram detailing the selection of patients included in the retrospective analysis.

Ministry of Health of the People's Republic of China [25]. Among them, 145 individuals were classified in the good prognosis group, and 153 in the poor prognosis group. The patient selection process is shown in **Figure 1**. All patients received RFA treatment. This study was approved by the ethics committee of Linyi People's Hospital.

Inclusion criteria: 1) Single tumors with a diameter ≤ 5 cm; 2) Multiple tumors with a diameter ≤ 3 cm and no more than 3 tumors; 3) No portal vein tumor thrombus, distant metastasis, or invasion of adjacent organs; 4) Child-Pugh class A or B, or those who meet this standard after liver protection treatment; 5) Single tumors > 5 cm or multiple tumors > 3 cm that are not amenable to surgical resection; 6) Patients aged ≥ 18 years without significant hearing impairment, vision impairment, or dementia before operation; 7) Patients with complete and standardized medical records, including current and past medical history, laboratory, and imaging examination results.

Exclusion criteria: 1) Giant tumors or diffuse HCC; 2) Tumors ≤ 3 cm with invasion of the main portal vein or its second branch, hepatic vein invasion, distant metastasis, or invasion of adjacent organs; 3) Tumors located on the surface of the liver with more than one-third of the tumor exposed; 4) Child-Pugh class C that can-

not be improved after liver-protective treatment; 5) Patients with esophagogastric variceal rupture and bleeding within 1 month before treatment; 6) Patients with coagulation disorders, uncorrectable abnormal blood counts, or significant bleeding tendencies; 7) Patients with refractory massive ascites or cachexia; 8) Patients with active infections, such as biliary system inflammation; 9) Patients with severe organ failure (liver, kidney, heart, lung, or brain); 10) Other conditions, such as impaired consciousness preventing cooperation with treatment.

Definition of Prognosis: Good prognosis was defined as patients who achieved complete tumor ablation during the first follow-up (confirmed by postoperative imaging) and remained disease-free during the follow-up period (up to December 31, 2023). Disease-free survival (DFS) was defined as the time from RFA to either intrahepatic recurrence, extrahepatic metastasis, or the last follow-up, with patients in this group showing no evidence of recurrence during this period. Poor prognosis was defined as patients who experienced recurrence, including intrahepatic tumor recurrence, extrahepatic metastasis, or local tumor progression, within the follow-up period. Recurrence was confirmed through imaging (MRI, CT, or ultrasound) and/or elevated serum biomarkers (AFP and AFP-L3). Additionally, incomplete tumor abla-

Serum biomarkers and MRI for hepatocellular carcinoma

tion observed in the first follow-up MRI was also categorized as a poor prognosis.

Data extraction

RFA treatment was performed using CT-guided percutaneous puncture with the Aquilion 16-row CT scanner and the Olympus Celon bipolar/multipolar radiofrequency ablation device. Before the procedure, all patients underwent routine MRI and MR-DWI to assess lesion characteristics (number, location, and extent). Laboratory parameters, including γ -glutamyl transpeptidase (γ -GT), platelet count (PLT), serum creatinine (SCr), albumin (Alb), neutrophil count (NEUT), monocyte count (MONO), AFP-L3 (%), and AFP (ng/mL), were measured one day before surgery and one week after surgery. These data were analyzed using standardized laboratory methods in the hospital's certified clinical laboratory: 1) γ -GT, SCr, Alb, PLT, NEUT, and MONO were measured with an automated biochemical analyzer (Roche Cobas 8000) using enzyme-coupled reaction assays and flow cytometry. 2) AFP and AFP-L3 levels were measured using chemiluminescent enzyme immunoassay (CLEIA) technology on the LUMIPULSE G1200 analyzer (Fujirebio Inc.).

Radiomics analysis consisted of manual segmentation of the volumetric regions of interest (VOI), feature extraction, model construction, and validation. Two experienced abdominal radiologists (with >10 years of experience in liver imaging) delineated the VOIs on seven MRI sequences (T1WI-FS, T2WI-FS, ADC, arterial phase, portal venous phase, transitional phase, and hepatobiliary phase) using 3D Slicer software. The radiologists independently segmented the tumor (VOItumor), surrounding regions (VOI10mm and VOI20mm), and a normal liver region (VOIiver), with final delineations determined by consensus.

Feature extraction was conducted using Py-Radiomics (version 3.0.1) to derive 5185 radiomics features per patient, including signal intensity, texture, and wavelet features. Feature selection was performed using univariate and multivariate logistic regression to identify relevant features, which were retained in a combined column-line chart model. The predictive performance of the model was validated using the training and validation datasets through receiver operating characteristic (ROC) analy-

sis, and calibration was assessed using calibration curves.

Follow-up protocols included serum AFP and AFP-L3 testing, chest CT, and abdominal CT or MR enhanced imaging every 3 months for 2 years and every 6 months thereafter. Disease-free survival (DFS) was defined as the time from RFA to intrahepatic recurrence, extrahepatic metastasis, or the last follow-up, ensuring that all patients completed follow-up by December 31, 2023.

Outcome measures

The gold standard for determining the true outcome of tumor treatment is histopathologic examination [26], which is the definitive diagnostic method when there is a suspicion of tumor residue in the ablation area, local tumor progression, or new intrahepatic tumor. However, in clinical practice, it is often not possible to perform biopsy for every suspected active tumor lesion. In this study, a comprehensive approach was used to assess lesions without biopsy, including imaging modalities (MRI, ultrasound, CT) and monitoring AFP and AFP-L3 levels. Confirmation was obtained through follow-up, and if a lesion showed progressive growth on consecutive imaging follow-up and there was a continuous increase in AFP and AFP-L3 levels, it was considered to be active tumor. Based on the standardized clinical application of image-guided liver tumor thermal ablation techniques, it was determined whether the lesion represented residual tumor, local tumor progression, or a new intrahepatic tumor.

Regarding the determination of complete ablation, histopathologic examination was not used for individual assessment. Instead, in the first postoperative follow-up, if no residual tumor was found, the tumor margin was evaluated for complete ablation by comparing pre-RFA and first post-RFA follow-up MRI. If the tumor margin was determined to be sufficiently ablated, it was considered complete ablation, which was further confirmed by subsequent follow-ups.

Statistical analysis

Categorical variables for patients in the training and validation groups were compared using the chi-square test or Fisher's exact test and are

Serum biomarkers and MRI for hepatocellular carcinoma

Table 1. Clinical characteristics

	Good prognosis group (n=145)	Poor prognosis group (n=153)	P
Gender			0.857
Male	80 (55.2%)	86 (56.2%)	
Female	65 (44.8%)	67 (43.8%)	
Age	70.5±5.0	69.2±7.8	0.088
BMI (kg/m ²)	26.0±3.6	25.7±2.0	0.291
Systolic pressure (mmHg)	127.7±4.5	128.8±5.4	0.068
Diastolic pressure (mmHg)	73.3±7.7	74.6±5.7	0.095
Coronary heart disease	62 (42.8%)	64 (41.8%)	0.871
Cardiac insufficiency	105 (72.4%)	128 (77.1%)	0.349
Renal insufficiency	15 (10.3%)	8 (5.2%)	0.098
Hyperthyroidism	3 (2.1%)	4 (2.6%)	0.756
Sleep apnea	6 (4.1%)	2 (1.3%)	0.131
Hypertension	105 (72.4%)	97 (63.4%)	0.096
Diabetes	32 (22.1%)	31 (20.2%)	0.702
Hyperlipidemia	128 (88.3%)	132 (86.3%)	0.605
Smoking	44 (30.3%)	57 (37.3%)	0.208
Drinking	20 (13.8%)	34 (22.2%)	0.059

presented as counts and percentages. Univariate logistic regression was performed to assess the predictive value of each feature in the training group for predicting RFA prognosis. Variables with a *p*-value <0.05 were included in the multivariate logistic regression analysis. A nomogram was developed using R (version 3.6.1; <http://www.r-project.org/>). The clinical net benefit of the model was evaluated using decision curve analysis. Survival curves were generated using the Kaplan-Meier method and compared using the log-rank test. Receiver operating characteristic (ROC) analysis, including the area under the ROC curve (AUC), was used to compare the predictive performance of the models. Statistical analyses were conducted with IBM SPSS Statistics (version 22, USA). A *p*-value <0.05 was considered significant.

Results

Comparison of clinical data between the two groups

Table 1 presents the characteristics of all subjects. A total of 298 patients with hepatocellular carcinoma (HCC) were included in this study, with 145 individuals in the good prognosis group (mean age 71.1±8.3 years) and 153 individuals in the poor prognosis group (mean age 64.3±10.4 years). There were no significant differences between the two groups in terms of

BMI, systolic blood pressure, diastolic blood pressure, or past medical history (all *P*>0.05). The two groups were comparable in terms of demographics and clinical characteristics (all *P*>0.05).

Comparison of serum AFP and AFP-L3 levels between the two groups

The levels of alpha-fetoprotein and AFP-L3 were compared between the good prognosis and poor prognosis groups before and after surgery (**Figure 2A** and **2B**). After surgery, AFP levels decreased significantly in both groups (*P*<0.05 for each), but the poor prognosis group still exhibited significantly higher AFP levels than the good prognosis group (*P*<0.05) (**Figure 2A**). A similar trend was observed for AFP-L3. After surgery, AFP-L3 levels decreased significantly in both groups (*P*<0.05 for each), but the poor prognosis group still had significantly higher AFP-L3 levels than the good prognosis group (*P*<0.05) (**Figure 2B**).

Comparison of magnetic resonance imaging radiomics between the two groups

Significant differences were observed between the two groups in terms of tumor diameter, intratumoral fat, intratumoral hemorrhage, and peritumoral low signal in the hepatobiliary phase (all *P*<0.05) (**Table 2**).

Serum biomarkers and MRI for hepatocellular carcinoma

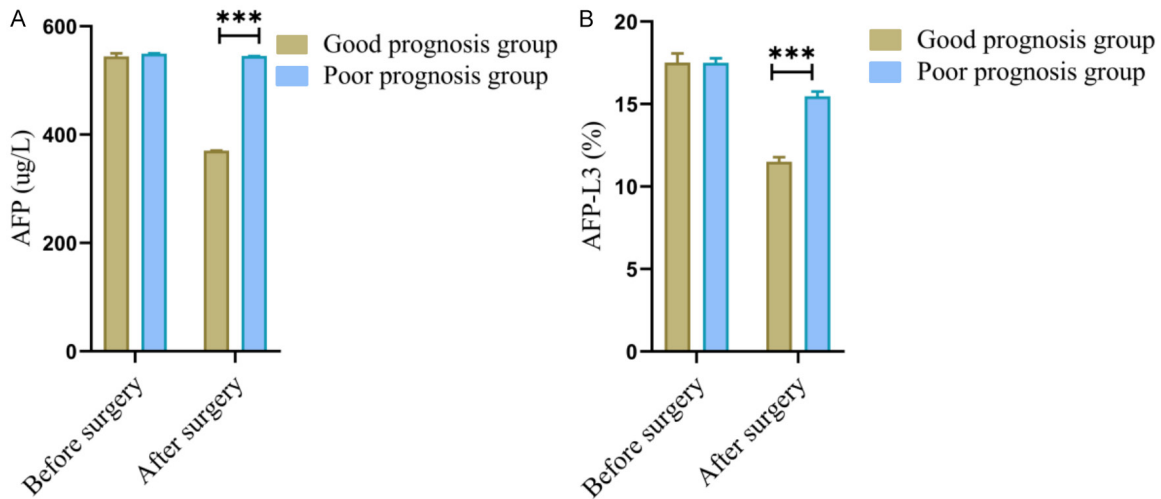


Figure 2. Comparison of serum AFP and AFP-L3 levels between the two groups before and after surgery. (A) AFP, (B) AFP-L3. AFP: alpha - fetoprotein; AFP-L3: lectin-reactive alpha-fetoprotein. Compared to the control group, *** $P < 0.001$.

Table 2. Comparison of magnetic resonance imaging radiomics between the two groups

	Good prognosis group (n=145)	Poor prognosis group (n=153)	P
Tumor diameter	2.04±0.59	3.79±0.45	0.000
Number of tumors	2.53±0.63	2.41±0.70	0.137
Envelope	62 (42.8%)	64 (41.8%)	0.871
Tumor margin	44 (30.3%)	57 (37.3%)	0.208
Intratumoral necrosis	20 (13.8%)	34 (22.2%)	0.059
Intratumoral fat	133.04±7.74	128.03±5.49	0.000
Intratumoral hemorrhage	32 (22.1%)	11 (20.2%)	0.000
Peritumoral enhancement during arterial phase	6 (4.1%)	2 (1.3%)	0.131
Peritumoral low signal in the hepatobiliary phase	105 (72.4%)	78 (51.0%)	0.000

Study population

A total of 160 eligible individuals were randomly divided into two groups (1:1 ratio) using computer-generated random numbers: 80 individuals were assigned to the training set and 80 to the validation set. The clinical characteristics of both sets are shown in **Table 3**. No significant differences were found between the two groups for most clinical, laboratory, and imaging parameters, indicating that the cohorts were well balanced. Among the demographic and clinical variables, the proportion of male (67.5%) and female (32.5%) patients was identical in both groups ($P=1.000$). Age distribution was similar, with 63.8% of patients aged ≤ 55 years and 36.2% aged > 55 years ($P=0.789$). Hepatitis B surface antigen (HBsAg) positivity was observed in 85.0% of patients in both groups ($P=$

0.675), and the proportions of patients with portal hypertension were comparable in the training (62.5%) and validation (60.0%) cohorts ($P=0.621$). The successful application of propensity score matching ensured comparability between the two cohorts across a range of clinical, laboratory, and imaging data. This balance enhanced the reliability of subsequent predictive modeling and analysis.

Univariate and multivariate analysis

Univariate and multivariate analyses identified predictive factors associated with poor prognosis after RFA for HCC (**Table 4**). Independent predictive factors included: AFP-L3 (95% CI -1.228, -1.1.61; $P < 0.001$), AFP (95% CI 0.017, 0.036; $P < 0.001$), intratumoral hemorrhage (95% CI 0.380, 0.581; $P < 0.001$), peritumoral

Serum biomarkers and MRI for hepatocellular carcinoma

Table 3. Characteristics of the training and validation sets

Data	Training set (n=80)	Validation set (n=80)	P value
Gender			0.738
Male	54 (67.5%)	52 (65.0%)	
Female	26 (32.5%)	28 (35.0%)	
Age			0.742
≤55	50 (62.5%)	52 (65.0%)	
>55	30 (37.5%)	28 (35.0%)	
HBsAg			0.339
Negative	12 (15.0%)	8 (10.0%)	
Positive	68 (85.0%)	72 (90.0%)	
Portal hypertension			0.746
Yes	50 (62.5%)	48 (60.0%)	
No	30 (37.5%)	32 (40.0%)	
AFP-L3			0.519
≤10	34 (42.5%)	30 (37.5%)	
>10	46 (57.5%)	50 (62.5%)	
AFP			0.750
≤200	34 (42.5%)	36 (45.0%)	
>200	46 (57.5%)	44 (55.0%)	
ALT			0.519
≤40	46 (57.5%)	50 (62.5%)	
>40	34 (42.5%)	30 (37.5%)	
AST			0.748
≤40	48 (60.0%)	46 (57.5%)	
>40	32 (40.0%)	34 (42.5%)	
TBiL			0.873
≤17.1	45 (56.2%)	46 (57.5%)	
>17.1	35 (43.8%)	34 (42.5%)	
PLT			0.751
≤100	42 (52.5%)	44 (55.0%)	
>100	38 (47.5%)	36 (45.0%)	
PT			0.750
≤13.1	36 (45.0%)	34 (42.5%)	
>13.1	44 (55.0%)	46 (57.5%)	
MR manifestation of tumor diameter			0.751
≤3	44 (55.0%)	42 (52.5%)	
>3	36 (45.0%)	38 (47.5%)	
Number of tumors			0.750
Single	46 (57.5%)	44 (55.0%)	
Multiple	34 (42.5%)	36 (45.0%)	
Envelope			0.751
Incomplete	42 (52.5%)	44 (55.0%)	
Complete	38 (47.5%)	36 (45.0%)	
Tumor margin			0.751
Smooth	44 (55.0%)	42 (52.5%)	
Unsmooth	36 (45.0%)	38 (47.5%)	
Intratatumoral fat			0.525
Yes	34 (42.5%)	38 (47.5%)	
No	46 (57.5%)	42 (52.5%)	

Serum biomarkers and MRI for hepatocellular carcinoma

Peritumoral enhancement during arterial phase			0.751
Yes	44 (55.0%)	42 (52.5%)	
No	36 (45.0%)	38 (47.5%)	

Note: HBsAg: Hepatitis B surface antigen; AFP-L3: lectin-reactive alpha-fetoprotein; AFP: Alpha - fetoprotein; ALT: Alanine Aminotransferase; AST: Aspartate Aminotransferase; TBil: Total Bilirubin; PLT: Platelet Count; PT: Prothrombin Time; MR: Magnetic Resonance.

Table 4. Univariate and multivariate logistic regression analysis

Data	Univariate analysis			Multivariate analysis		
	OR	95% CI	P	OR	95% CI	P
AFP-L3	1.312	-0.674, 1.324	0.044	46.127	-1.228, -1.1.61	0.000
AFP	2.469	-0.764, 0.714	0.026	5.564	0.017, 0.036	0.000
Tumor diameter	1.003	-0.984, 0.874	1.001			
Number of tumors	0.957	0.694, 3.795	0.912			
Envelope integrity	4.654	0.544, 2.174	0.002	0.162	-0.125, 0.106	0.872
Intratumoral necrosis	1.961	-0.789, 1.678	0.112			
Intratumoral fat	1.562	-0.016, 1.487	0.451			
Intratumoral hemorrhage	1.962	-0.164, 1.498	0.113	9.403	0.380, 0.581	0.000
Peritumoral enhancement of arterial tumors	4.652	0.754, 2.364	0.001	4.202	0.193, 0.534	0.000
Low signal intensity around liver and gallbladder tumors	2.635	0.225, 1.764	0.012	6.702	0.267, 0.489	0.000
Cirrhosis	1.926	-0.347, 1.654	0.187			

Note: AFP-L3: lectin-reactive alpha-fetoprotein; AFP: Alpha - fetoprotein.

arterial tumor enhancement (95% CI 0.193, 0.534; $P < 0.001$) and low signal intensity around liver and gallbladder tumors (95% CI 0.267, 0.489; $P < 0.001$).

Number of selected features in a single sequence

In this study, we selected the best 4 clinical and radiologic data and 12 radiomic features. We established three models: a radiomics model, clinical-radiomics model, and clinical-radiological-radiomics model (**Table 5**).

Predictive performance of individual sequences

Individual sequence results showed that T1WI-FS had a higher AUC (0.874 vs. 0.798, training group vs. validation group) and hepatobiliary phase had a higher AUC (0.863 vs. 0.756, training group vs. validation group) compared to other sequences (**Table 6**). Features extracted from both the training and validation groups outperformed those from T2WI-FS, ADC, arterial phase, portal venous phase, and transitional phase. To further validate the differences in AUCs, we conducted statistical comparisons using the DeLong test.

Discussion

To predict the prognosis of hepatocellular carcinoma (HCC) patients after RFA, this study established and validated a predictive model using a multi-modal imaging radiomic nomogram that incorporated post-RFA serum AFP and AFP-L3 levels. The model identified independent risk factors for post-RFA prognosis, including AFP, AFP-L3, capsule integrity, arterial phase tumor enhancement, radiomic vascular imaging (RVI), and radiomics score. The nomogram demonstrated satisfactory performance in both the training and validation groups. Calibration curves showed good consistency between predicted and actual probabilities. Moreover, the model's prediction of time to recurrence was consistent with histopathologic results.

The measurement of serum AFP and AFP-L3 concentrations is a widely used method for screening HCC and plays a significant role in predicting prognosis [27]. Elevated AFP and AFP-L3 concentrations have been shown to predict poor prognosis after RFA in HCC patients [28, 29], consistent with the findings of this study. Specifically, this study identified an AFP concentration >200 ng/mL as an indepen-

Serum biomarkers and MRI for hepatocellular carcinoma

Table 5. Number of selected features in a single sequence

Sequence	Total number of features	Univariate feature selection	Selection of intra group correlation coefficients	mRMR	LASSO selection	Multivariate logistic regression selection
T1WI-FS	5185	410	160	20	10	10
T2WI-FS	5185	525	168	20	10	10
ADC	5185	428	190	20	8	8
Arterial phase	5185	620	249	20	8	7
Portal venous phase	5185	375	171	20	8	7
Migration period	5185	248	130	20	8	8
Hepatobiliary phase	5185	198	85	20	9	9

Note: mRMR: minimum redundancy and maximum correlation; LASSO: minimum absolute shrinkage and selection operator; T1WI - FS: T1 - weighted imaging with fat suppression; T2WI - FS: T2 - weighted imaging with fat suppression; ADC: Apparent Diffusion Coefficient.

Table 6. Efficiency of predicting prognosis by extracting features from different sequences

Sequence	Training group				Verification group			
	AUC	Accuracy	Susceptibility	Specificity	AUC	Accuracy	Susceptibility	Specificity
T1WI-FS	0.874 (0.835-0.931)	0.783	0.789	0.772	0.823 (0.769-0.864)	0.798	0.694	0.853
T2WI-FS	0.789 (0.746-0.832)	0.712	0.803	0.632	0.746 (0.712-0.769)	0.703	0.756	0.637
ADC	0.801 (0.778-0.832)	0.763	0.751	0.762	0.664 (0.597-0.763)	0.647	0.586	0.664
Arterial phase	0.796 (0.765-0.843)	0.736	0.745	0.723	0.726 (0.698-0.769)	0.723	0.657	0.756
Portal venous phase	0.712 (0.706-0.789)	0.698	0.762	0.632	0.736 (0.698-0.785)	0.697	0.765	0.637
Migration period	0.795 (0.779-0.826)	0.762	0.736	0.748	0.726 (0.687-0.768)	0.746	0.856	0.698
Hepatobiliary phase	0.863 (0.825-0.896)	0.775	0.697	0.856	0.762 (0.722-0.806)	0.756	0.687	0.789

Note: AUC is displayed with a 95% confidence interval. T1WI - FS: T1 - weighted imaging with fat suppression; T2WI - FS: T2 - weighted imaging with fat suppression; ADC: Apparent Diffusion Coefficient.

dent risk factor for poor prognosis after RFA. Other studies have suggested that AFP levels above 400 ng/mL are important predictors of poor prognosis [30]. In conclusion, elevated AFP and AFP-L3 concentrations are key indicators of poor prognosis following RFA. Incomplete capsule formation is another critical predictor, since it is associated with tumor differentiation and immune suppression [31]. Poor differentiation and rapid proliferation hinder the formation of a complete tumor capsule, facilitating tumor spread. Additionally, immune suppression weakens the surrounding tissue's anti-tumor effects, further preventing capsule formation [32].

This study identified RVI as an independent predictive factor for poor prognosis after RFA in HCC. Research suggests that RVI biomarkers, which correlate imaging features with gene characteristics, may have broad clinical applicability. The model demonstrated an accuracy of 89%, sensitivity of 76%, and specificity of 94% in predicting poor prognosis after RFA [33]. The imaging features of RVI consist of three independent characteristics: intratumoral arteries, peritumoral low attenuation rim, and tumor-liver density/signal difference. Intratumoral arteries are small vessels within the tumor that exhibit persistent enhancement during the arterial phase. Their presence indicates angiogenesis driven by cell factors produced by tumor and stromal cells, which leads to increased tumor vascularization and is associated with a unique HCC molecular subtype, heightened cell proliferation, matrix invasion, and poor prognosis after RFA. The peritumoral low attenuation rim appears as a low attenuation edge surrounding the tumor during the portal venous or transitional phase. This phenomenon is likely due to liver tissue fibrosis at the tumor's edge caused by tumor expansion and compression. Tumor-liver density/signal difference refers to the signal difference between the tumor and adjacent liver parenchyma, without a low attenuation halo. The relationship between RVI, poor prognosis after RFA, and molecular spectra may allow future reconstruction of gene expression in HCC using imaging methods.

However, liver cirrhosis may affect the accuracy of RVI in predicting poor prognosis after RFA, as it affects the risk of HCC recurrence due to underlying liver disease. Cirrhosis may also alter RVI scoring and tumor biology, making RVI

less sensitive for predicting microvascular invasion (MVI) [34]. Despite this, our study found RVI to be an independent risk factor for MVI, and combining gene markers with imaging features can enhance the prediction of prognosis after RFA in HCC patients.

The rapid advancement of radiomics offers more detailed quantitative insight into tumor biology and the tumor microenvironment, complementing traditional morphologic features [35]. Accurate delineation of the region of interest (ROI) is crucial for radiomic analysis. Unlike previous MR radiomic studies, this study used three-dimensional data encompassing the entire ROI. Compared to two-dimensional delineation, three-dimensional delineation better reflects the tumor's overall contour and allows for a more detailed and reproducible quantitative assessment of tumor characteristics. Studies have shown that feature extraction based on the maximum cross-sectional area in two-dimensional ROIs cannot fully represent the entire tumor [36]. Thus, the multi-region, multi-sequence, three-dimensional radiomic features in this study more accurately reflect the complete tumor information, leading to more objective predictive results.

Different MR sequences have shown varying predictive effects on poor prognosis after RFA, which is likely influenced by study design and sample size. In a previous study, a radiomic model based on T1WI, T2WI, DWI, arterial phase, portal venous phase, and transitional phase achieved AUC values of 0.778 and 0.803 for the training and validation groups, respectively [37]. In contrast, this study incorporated the hepatobiliary phase and achieved higher AUC values in both groups. This suggests that including more MR sequences improves the predictive ability for poor prognosis after RFA.

This study has some limitations. The data were obtained from a single center, and the study population was relatively small. Future studies should expand the cohort and include various stages of hepatic cell carcinoma thermal ablation to further validate these findings.

In conclusion, this study developed and validated a clinical-radiomic nomogram model, incorporating serum AFP, AFP-L3, and radiomic features, to predict poor prognosis in HCC patients undergoing RFA.

Disclosure of conflict of interest

None.

Address correspondence to: Jinghua Liu, Department of General Surgery Center, Linyi People's Hospital, No. 27 of Jiefang East Road, Linyi 276000, Shandong, P. R. China. Tel: +86-0539-8221087; E-mail: jinghualiu_1982@163.com; Fenghua Zhang, Department of Operating Room, Linyi People's Hospital, Linyi 276000, Shandong, P. R. China. Tel: +86-0539-8221087; E-mail: 17661667766@139.com

References

- [1] Rumgay H, Arnold M, Ferlay J, Lesi O, Cabasag CJ, Vignat J, Laversanne M, McGlynn KA and Soerjomataram I. Global burden of primary liver cancer in 2020 and predictions to 2040. *J Hepatol* 2022; 77: 1598-1606.
- [2] Jan J, Osho A, Murphy CC, Mazure CM, Singal AG and Rich NE. Gender, age, racial and ethnic disparities in clinical trial enrollment for primary liver cancer. *Gastroenterology* 2022; 163: 14-20, e2.
- [3] Lin J, Zhang H, Yu H, Bi X, Zhang W, Yin J, Zhao P, Liang X, Qu C, Wang M, Hu M, Liu K, Wang Y, Zhou Z, Wang J, Tan X, Liu W, Shao Z, Cai J, Tang W and Cao G. Epidemiological characteristics of primary liver cancer in mainland China from 2003 to 2020: a representative multicenter study. *Front Oncol* 2022; 12: 906778.
- [4] Cao M, Ding C, Xia C, Li H, Sun D, He S and Chen W. Attributable deaths of liver cancer in China. *Chin J Cancer Res* 2021; 33: 480-489.
- [5] Liu Z, Mao X, Jiang Y, Cai N, Jin L, Zhang T and Chen X. Changing trends in the disease burden of primary liver cancer caused by specific etiologies in China. *Cancer Med* 2019; 8: 5787-5799.
- [6] Gao Y, Xi H, Shang L, Tang Z, Wei B, Qiao Z, Tang Y, Wang X, Zhou J, Wang X, Huang C, Lu J, Li G, Yu J, Liang Y, Ji J, Li Z, Xue K, Liang H, Ke B, Zang L, He Z, Xie S, Huang H, Xu Z, Tian Y, Xiong J, Li J, Cui Q, Li L, Lu T, Song Q, Liu S, Sun Y, Li L and Chen L. Clinical landscape and prognosis of patients with gastric cancer liver metastases: a nation-wide multicenter cohort study in China (RECORD study). *Sci Bull (Beijing)* 2024; 69: 303-307.
- [7] Hao D, Yong RJ, Cohen SP and Stojanovic MP. Medial branch blocks and radiofrequency ablation for low back pain from facet joints. *N Engl J Med* 2023; 389: e53.
- [8] Stewart KA, Greenberg JA, Kho KA and Cohen Rassier SL. Radiofrequency ablation of leiomyomas. *Obstet Gynecol* 2023; 141: 1063-1071.
- [9] Tang Z, Kang M, Zhang B, Chen J, Fang H, Ye Q, Jiang B and Wu Y. Advantage of sorafenib combined with radiofrequency ablation for treatment of hepatocellular carcinoma. *Tumori* 2017; 103: 286-291.
- [10] Oeda S, Mizuta T, Isoda H, Kuwashiro T, Iwane S, Takahashi H, Kawaguchi Y, Eguchi Y, Ozaki I, Tanaka K and Fujimoto K. Survival advantage of radiofrequency ablation for hepatocellular carcinoma: comparison with ethanol injection. *Hepatogastroenterology* 2013; 60: 1399-1404.
- [11] Liu PH, Lee YH, Hsu CY, Huang YH, Chiou YY, Lin HC and Huo TI. Survival advantage of radiofrequency ablation over transarterial chemoembolization for patients with hepatocellular carcinoma and good performance status within the Milan criteria. *Ann Surg Oncol* 2014; 21: 3835-3843.
- [12] Atiç R, Alemdar C, Elçi S, Dusak A, Çağan MA, Özkul E and Aytekin MN. Comparative analysis of percutaneous excision and radiofrequency ablation for osteoid osteoma. *Med Sci Monit* 2023; 29: e940292.
- [13] Tang Y, Shu Z, Zhu M, Li S, Ling Y, Fu Y, Hu Z, Wang J, Yang Z, Liao J, Xu L, Yu M and Peng Z. Size-tunable nanoregulator-based radiofrequency ablation suppresses MDSCs and their compensatory immune evasion in hepatocellular carcinoma. *Adv Healthc Mater* 2023; 12: e2302013.
- [14] Kan X, Zhou G, Zhang F, Ji H, Zheng H, Chick JF, Valji K, Zheng C and Yang X. Interventional optical imaging permits instant visualization of pathological zones of ablated tumor periphery and residual tumor detection. *Cancer Res* 2021; 81: 4594-4602.
- [15] Zhang S, Huang Y, Pi S, Chen H, Ye F, Wu C, Li L, Ye Q, Lin Y and Su Z. Autophagy-amplifying nanoparticles evoke immunogenic cell death combined with anti-PD-1/PD-L1 for residual tumors immunotherapy after RFA. *J Nanobiotechnology* 2023; 21: 360.
- [16] Zhou Y, Liu X, Zhang W, Xu Y, Zhang Q, Xiong S, Tang H and Luo B. HMGB1 released from dead tumor cells after insufficient radiofrequency ablation promotes progression of HCC residual tumor via ERK1/2 pathway. *Int J Hyperthermia* 2023; 40: 2174709.
- [17] Li J, Zhou K, Wu M, Zhang R, Jin X, Qiao H, Li J, Cao X, Zhang S and Dong G. The characteristics of transcription factors regulating T cell exhaustion were analyzed to predict the prognosis and therapeutic effect in patients with HCC. *Int J Gen Med* 2023; 16: 5597-5619.
- [18] Chalasani NP, Ramasubramanian TS, Bhatnagary A, Olson MC, Edwards V DK, Roberts LR, Kisiel JB, Reddy KR, Lidgard GP, Johnson

Serum biomarkers and MRI for hepatocellular carcinoma

- SC and Bruinsma JJ. A novel blood-based panel of methylated DNA and protein markers for detection of early-stage hepatocellular carcinoma. *Clin Gastroenterol Hepatol* 2021; 19: 2597-2605, e4.
- [19] Tian S, Chen Y, Zhang Y and Xu X. Clinical value of serum AFP and PIVKA-II for diagnosis, treatment and prognosis of hepatocellular carcinoma. *J Clin Lab Anal* 2023; 37: e24823.
- [20] Liu Y, Han G, Gong J, Hua X, Zhu Q, Zhou S, Jiang L, Li Q, and Liu S. Intramolecular fluorescence resonance energy transfer strategy for accurate detection of AFP-L3% and improved diagnosis of hepatocellular carcinoma. *Spectrochim Acta A Mol Biomol Spectrosc* 2023; 300: 122950.
- [21] Huang C, Xiao X, Zhou L, Chen F, Wang J, Hu X and Gao C. Chinese expert consensus statement on the clinical application of AFP/AFP-L3%/DCP using GALAD and GALAD-like algorithm in HCC. *J Clin Lab Anal* 2023; 37: e24990.
- [22] Guo H, Tang HT, Hu WL, Wang JJ, Liu PZ, Yang JJ, Hou SL, Zuo YJ, Deng ZQ, Zheng XY, Yan HJ, Jiang KY, Huang H, Zhou HN and Tian D. The application of radiomics in esophageal cancer: predicting the response after neoadjuvant therapy. *Front Oncol* 2023; 13: 1082960.
- [23] Zhang HW, Huang DL, Wang YR, Zhong HS and Pang HW. CT radiomics based on different machine learning models for classifying gross tumor volume and normal liver tissue in hepatocellular carcinoma. *Cancer Imaging* 2024; 24: 20.
- [24] Zhuang BW, Li W, Qiao B, Zhang N, Lin MX, Wang W, Kuang M, Lu MD, Xie XY and Xie XH. Preoperative prognostic value of alpha-fetoprotein density in patients with hepatocellular carcinoma undergoing radiofrequency ablation. *Int J Hyperthermia* 2022; 39: 1143-1151.
- [25] Zhou J, Sun H, Wang Z, Cong W, Wang J, Zeng M, Zhou W, Bie P, Liu L, Wen T, Han G, Wang M, Liu R, Lu L, Ren Z, Chen M, Zeng Z, Liang P, Liang C, Chen M, Yan F, Wang W, Ji Y, Yun J, Cai D, Chen Y, Cheng W, Cheng S, Dai C, Guo W, Hua B, Huang X, Jia W, Li Y, Li Y, Liang J, Liu T, Lv G, Mao Y, Peng T, Ren W, Shi H, Shi G, Tao K, Wang W, Wang X, Wang Z, Xiang B, Xing B, Xu J, Yang J, Yang J, Yang Y, Yang Y, Ye S, Yin Z, Zhang B, Zhang B, Zhang L, Zhang S, Zhang T, Zhao Y, Zheng H, Zhu J, Zhu K, Liu R, Shi Y, Xiao Y, Dai Z, Teng G, Cai J, Wang W, Cai X, Li Q, Shen F, Qin S, Dong J and Fan J. Guidelines for the diagnosis and treatment of hepatocellular carcinoma (2019 edition). *Liver Cancer* 2020; 9: 682-720.
- [26] Mohammed AF, Chen X and Li C. Clinical utility of biomarkers of hepatocellular carcinoma. *Bratisl Lek Listy* 2024; 125: 102-106.
- [27] Chen Y, Chen Y, Ning W, Zhang W, Li L, Wang X, Yin Y and Zhang H. Diagnostic value of maternal alpha-fetoprotein variants in second-trimester biochemical screening for trisomy 21 and 18. *Sci Rep* 2022; 12: 13605.
- [28] Zhou J, Zhu Y, Li Y, Liu K, He F, Xu S, Li X, Li L, Hu J and Liu Y. Combined detection of circulating tumor cells, alpha-fetoprotein heterogene-3 and alpha-fetoprotein in the early diagnosis of HCC for the prediction of efficacy, prognosis, recurrence after microwave ablation. *Infect Agent Cancer* 2021; 16: 28.
- [29] Takada H, Tsuchiya K, Yasui Y, Nakakuki N, Tamaki N, Suzuki S, Nakanishi H, Itakura J, Takahashi Y, Kurosaki M, Asahina Y, Enomoto N and Izumi N. Irregular vascular pattern by contrast-enhanced ultrasonography and high serum Lens culinaris agglutinin-reactive fraction of alpha-fetoprotein level predict poor outcome after successful radiofrequency ablation in patients with early-stage hepatocellular carcinoma. *Cancer Med* 2016; 5: 3111-3120.
- [30] Yao LQ, Fan ZQ, Wang MD, Diao YK, Chen TH, Zeng YY, Chen Z, Wang XM, Zhou YH, Li J, Fan XP, Liang YJ, Li C, Shen F, Lv GY and Yang T. Prognostic value of serum alpha-fetoprotein level as an important characteristic of tumor biology for patients undergoing liver resection of early-stage hepatocellular carcinoma (BCLC Stage O/A): a large multicenter analysis. *Ann Surg Oncol* 2024; 31: 1219-1231.
- [31] Takahashi M, Wada T, Nakae R, Fujiki Y, Kanaya T, Takayama Y, Suzuki G, Naoe Y and Yokobori S. Antithrombin activity levels for predicting long-term outcomes in the early phase of isolated traumatic brain injury. *Front Immunol* 2022; 13: 981826.
- [32] Liu Y, Xu D, Liu Y, Zheng X, Zang J, Ye W, Zhao Y, He R, Ruan S, Zhang T, Dong H, Li Y and Li Y. Remotely boosting hyaluronidase activity to normalize the hypoxic immunosuppressive tumor microenvironment for photothermal immunotherapy. *Biomaterials* 2022; 284: 121516.
- [33] Nakai M, Morikawa K, Hosoda S, Yoshida S, Kubo A, Tokuchi Y, Kitagataya T, Yamada R, Ohara M, Sho T, Suda G, Ogawa K and Sakamoto N. Pre-sarcopenia and Mac-2 binding protein glycosylation isomer as predictors of recurrence and prognosis of early-stage hepatocellular carcinoma. *World J Hepatol* 2022; 14: 1480-1494.
- [34] Hasan I, Nababan SH, Handayu AD, Aprilicia G and Gani RA. Scoring system for predicting 90-day mortality of in-hospital liver cirrhosis patients at Cipto Mangunkusumo Hospital. *BMC Gastroenterol* 2023; 23: 190.
- [35] Limkin EJ, Sun R, Derclé L, Zacharaki EI, Robert C, Reuzé S, Schernberg A, Paragios N,

Serum biomarkers and MRI for hepatocellular carcinoma

- Deutsch E and Ferté C. Promises and challenges for the implementation of computational medical imaging (radiomics) in oncology. *Ann Oncol* 2017; 28: 1191-1206.
- [36] Li Y, Yang L, Gu X, Wang Q, Shi G, Zhang A, Yue M, Wang M and Ren J. Computed tomography radiomics identification of T1-2 and T3-4 stages of esophageal squamous cell carcinoma: two-dimensional or three-dimensional? *Abdom Radiol (NY)* 2024; 49: 288-300.
- [37] Hu F, Zhang Y, Li M, Liu C, Zhang H, Li X, Liu S, Hu X and Wang J. Preoperative prediction of microvascular invasion risk grades in hepatocellular carcinoma based on tumor and peritumor dual-region radiomics signatures. *Front Oncol* 2022; 12: 853336.